

**Balancing antiviral potency and host toxicity: identifying a nucleotide inhibitor
with an optimal kinetic phenotype for HIV-1 reverse transcriptase**

Christal D. Sohl, Rajesh Kasiviswanathan, Jiae Kim, Ugo Pradere, Raymond F. Schinazi,
William C. Copeland, Hiroaki Mitsuya, Masanori Baba, and Karen S. Anderson

Department of Pharmacology, Yale University, New Haven, CT, 06520, USA (C.D.S., J.K., K.S.A.), Laboratory of Molecular Genetics, National Institute of Environmental Health Sciences, National Institutes of Health, Research Triangle Park, NC, 27709, USA (R.K., W.C.C.), Center for AIDS Research, Department of Pediatrics, Emory University School of Medicine and Department of Veterans Affairs, Atlanta, GA, 30322, USA (U.P., R.F.S.), Departments of Infectious Diseases and Hematology, Kumamoto University Graduate School of Medical Sciences, Kumamoto, 860-8556, Japan (H.M.), Experimental Retrovirology Section, HIV and AIDS Malignancy Branch, National Cancer Institute, National Institutes of Health, Bethesda, MD, 20892, USA (H.M.), Division of Antiviral Chemotherapy, Center for Chronic Viral Diseases, Graduate School of Medical and Dental Sciences, Kagoshima University, Kagoshima, 890-8544, Japan (M.B.)

Running title:

A potent anti-HIV thymidine analog with low host toxicity

Corresponding author:

Dr. Karen S. Anderson; Department of Pharmacology, Yale University, New Haven, CT, 06520, USA. Phone: (203) 785 4536; Fax: (203) 785 7670; E-mail: karen.anderson@yale.edu

Number of text pages: 20

Number of Tables: 2

Number of Figures: 7

Number of references: 54

Number of words – Abstract: 250

Number of words – Introduction: 750

Number of words – Discussion: 1,487

Non-standard abbreviations: AZT, zidovudine; NRTI, nucleoside reverse transcriptase inhibitor; HIV-1, human immunodeficiency virus 1; FLT, 3'-fluoro-3'-deoxythymidine; Ed4T, 2',3'-didehydro-3'-deoxy-4'-ethynylthymidine, festinavir; WT, wild type; RT, WT HIV-1 reverse transcriptase; pol γ , human mitochondrial DNA polymerase γ , exonuclease deficient; exo⁺ pol γ , human mitochondrial DNA polymerase polymerase γ , exonuclease competent; dT, thymidine; TP, triphosphate; MP, monophosphate; d4T, stavudine, 2'-3'-didehydro-2'-3'-dideoxythymidine; R964C pol γ , human mitochondrial DNA polymerase γ catalytic subunit mutation R964C; PAGE; polyacrylamide gel electrophoresis.

Abstract

Two novel thymidine analogs, 3'-fluoro-3'-deoxythymidine (FLT) and 2',3'-dideoxy-3'-deoxy-4'-ethynylthymidine (Ed4T), have been investigated as nucleoside reverse transcriptase inhibitors (NRTIs) for treating HIV infection. Ed4T, in Phase II clinical trials, appears very promising, while toxicity halted FLT during this Phase. To understand these different molecular mechanisms of toxicity, pre-steady-state kinetics were used to examine the interactions of FLT and Ed4T with wild type human mitochondrial DNA polymerase γ (WT pol γ), which is often associated with NRTI toxicity, as well as the viral target protein, WT HIV-1 reverse transcriptase (RT). We report Ed4T-TP to be the first analog preferred over native nucleotides by RT but have negligible incorporation by WT pol γ , showing an ideal balance between high antiretroviral efficacy and minimal host toxicity. WT pol γ could discriminate Ed4T-TP from dTTP 12,000-fold better than RT, with only a 8.3-fold difference seen in discrimination for FLT-TP. A structurally related NRTI, d4T, is the only other analog favored by RT over native nucleotides, but it has only a 13-fold difference (versus 12,000 for Ed4T) in discrimination between the two enzymes. We propose the 4'-ethynyl group of Ed4T serves as an enzyme selectivity moiety, critical for discerning between RT and WT pol γ . We also show the pol γ mutation R964C, which predisposes HIV patients taking d4T to mitochondrial toxicity, showed some loss of discrimination for FLT-TP and Ed4T-TP. These molecular mechanisms of analog incorporation, which are critical for understanding pol γ -related toxicity, shed light on the unique toxicity profiles observed during clinical trials.

Introduction

Since the development of AZT in 1985 (Mitsuya et al., 1985), NRTIs have been vital in treating HIV infection. NRTIs inhibit RT by serving as nucleoside mimics; subsequent to phosphorylation by cellular kinases, the inhibitor is incorporated into DNA during reverse transcription. Currently available NRTIs lack a 3'-hydroxyl group, so incorporation causes immediate termination of polymerization. Despite the success of NRTIs, limitations include acquired resistance to RT, and host toxicity that can manifest as neuropathy, lactic acidosis, and hepatotoxicity (Apostolova et al., 2011).

Although some toxicity can be attributed to mechanisms such as phosphorylation inhibition (Apostolova et al., 2011), the primary cause of NRTI toxicity is via inhibition of pol γ (Koczor and Lewis, 2010; Kohler and Lewis, 2007). Pol γ , which replicates the human mitochondrial genome, is a heterotrimer containing a catalytic monomer with polymerization and exonuclease domains, and an accessory homodimer that improves incorporation efficiency and processivity (Johnson et al., 2000; Lee et al., 2009). Pol γ is a member of the A family of DNA polymerases, which are most similar to RT due to fold commonalities and conserved active site residues (Bienstock and Copeland, 2004). Thus, pol γ is more prone to insert NRTIs during replication and side effects are often indicators of mitochondrial toxicity (Brinkman et al., 1999).

The dT analog NRTIs AZT and d4T have been FDA-approved to treat HIV infection but are plagued by toxicity (Lee et al., 2003), highlighting the need for safer NRTIs. Two dT analogs, FLT and Ed4T, have been under investigation (Fig. 1). *In vitro* work showed FLT inhibited viral replication more effectively than AZT (Kong et al., 1992), with slow evolution of FLT-resistant mutations in RT (Kim et al., 2001). However,

FLT-treated rats had mitochondrial DNA depletion (Venhoff et al., 2009). Patient toxicity, including 2 deaths from hepatic failure, halted clinical trials in Phase II (Flexner et al., 1994). Interest in FLT has renewed somewhat with reports that FLT is effective at lower, less toxic doses (De Clercq, 2010). Phase II clinical trials with Ed4T have proved more promising despite its structural similarity to d4T (lacking the 4'-ethynyl), a relatively toxic NRTI which inhibits pol γ (Bailey et al., 2009; Johnson et al., 2001). *In vitro* studies showed Ed4T is 5 \times more potent and significantly less toxic than d4T (Dutschman et al., 2004; Painsil et al., 2007), and development of RT resistance is slow (Yang et al., 2009).

Despite documented mitochondrial toxicity for FLT and potential for mitochondrial toxicity for Ed4T due to structural similarity to d4T, studies directly probing their interactions with pol γ relative to RT are limited. Often NRTI potency comes at the expense of toxicity from increased WT pol γ inhibition, so both limited analog incorporation by WT pol γ and efficient incorporation by RT are vital. The ideal balance of potency and toxicity is more efficient analog incorporation versus native nucleotides by RT, and negligible analog incorporation by WT pol γ . However, this has not yet been achieved.

Previous steady-state studies have shown FLT-TP and Ed4T-TP interact with RT and WT pol γ . Unfortunately, steady-state experiments only provide information on the rate-limiting step of catalysis. For these two polymerases, the rate of polymerization is masked by the slow product-release step. A complete characterization of the analog kinetic profiles is needed, which includes the analog affinity and incorporation rates for both enzymes, and the analog removal rates by pol γ . Pre-steady-state kinetics were required to generate these molecular mechanisms of toxicity, which correspond well to

the degree of mitochondrial toxicity observed in patients (Johnson et al., 2001). We also examined the R964C pol γ mutant since patients with this mutation, located in the polymerase domain of the pol γ catalytic subunit, have higher instances of mitochondrial toxicity when taking d4T (Yamanaka et al., 2007).

We found WT pol γ was 1,400-fold better at distinguishing Ed4T-TP from dTTP than FLT-TP from dTTP, and this specificity was moderately impaired in R964C pol γ . Conversely, RT preferred Ed4T-TP to FLT-TP and dTTP. Importantly, Ed4T-TP is the first analog to show this exemplary balance of preferred incorporation by RT and negligible incorporation by WT pol γ . We propose the didehydro ring of Ed4T (and d4T) is important for achieving impaired discrimination in RT, while the 4'-ethynyl group serves as an enzyme selectivity moiety that supports the high discrimination by WT pol γ . The unique kinetic mechanisms of interaction for FLT and Ed4T can help explain the high levels of toxicity observed for FLT, and predict lower toxicity for Ed4T.

Materials and Methods

Reagents. The dTTP was purchased from GE Healthcare (Waukesha, WI). Triphosphate versions of FLT and Ed4T were prepared as described previously (Ray et al., 2002c). The DNA oligonucleotides D22 (5'-GCC TCG CAG CCG TCC AAC CAA C-3') and D45 (3'-CGG AGC GTC GGC AGG TTG GTT GAG TTG GAG CTA GGT TAC GGC AGG-5') were purchased from IDT (Coralville, IA) and were further purified on a 20% polyacrylamide denaturing gel. T4 polynucleotide kinase (New England Biolabs, Ipswich, MA) was used to label the D22 oligonucleotide at the 5' terminus with [γ -³²P] ATP (Perkin Elmer, Waltham, MA). This D22 primer was then annealed to the D45 template as described previously (Ray et al., 2002a) to generate the DNA primer/template substrate.

Enzymes. The recombinant WT accessory subunit of pol γ was expressed and purified as described elsewhere (Johnson et al., 2000). All pol γ catalytic subunits used contained an *N*-terminal hexa-histidine tag. The recombinant exonuclease-deficient WT catalytic subunit (WT pol γ) was expressed and purified as described previously (Graziewicz et al., 2004), with minor modifications in the chromatography strategy. Specifically, WT pol γ was eluted from a nickel column using a 20 to 400 mM imidazole linear gradient. The recombinant exonuclease-competent pol γ catalytic subunit (exo⁺ pol γ) was expressed and purified as described previously (Kasiviswanathan et al., 2010; Lim et al., 2003; Longley et al., 1998). Site-directed mutagenesis was used to generate the R964C pol γ construct (detailed in (Kasiviswanathan et al., 2010)), and the recombinant protein was expressed and purified as detailed elsewhere (Kasiviswanathan et al., 2010).

The recombinant RT (p66/p51 heterodimer) clone was kindly provided by Drs.

Stephen Hughes and Andrea Ferris (Frederick Cancer Research and Development Center, MD). The C-terminal hexa-histidine-tagged RT was purified as previously described (Kerr and Anderson, 1997; Kim et al., 2012). The purity for all proteins, as judged by SDS-PAGE analysis with Coomassie staining, was > 90%.

Single nucleotide incorporation assays. Single nucleotide incorporation experiments were performed using a KinTek RQF-3 rapid chemical quench apparatus (KinTek Corporation, Austin, TX) operated at 37°C. In order to determine the active site concentration of each of the enzymes used, dTTP incorporation into the D22/D45 primer/template substrate was examined under burst conditions as described previously (Murakami et al., 2003). Single-turnover conditions were used to examine the rate of dTTP, FLT-TP, and Ed4T-TP incorporation. For incorporation by WT pol γ and R964C pol γ , 100 nM (active site concentration) of pol γ catalytic subunit was preincubated with an excess of pol γ accessory subunit (4-fold higher than the total, not active site, concentration of the catalytic subunit). The 100 nM holoenzyme (the heterotrimer) and 25 nM DNA primer/template substrate in pol γ reaction buffer (50 mM Tris, pH 7.8 at 37°C, and 100 mM NaCl) was rapidly mixed with 2.5 mM MgCl₂ and varying concentrations of dTTP or analog. Single nucleotide incorporation experiments with RT were performed in the same fashion as the pol γ experiments, except 100 nM of RT was used instead of pol γ holoenzyme. Concentrations are final (post-mixing). After pre-steady-state time frames, the reactions were quenched with 0.3 M EDTA (pH 8.0) and the products were separated on a 0.4 mm thick 20% polyacrylamide denaturing gel (8 M urea). After quantitation by phosphorimaging using a Bio-Rad Molecular Imager FX (Hercules, CA), Kaleidagraph software (Synergy, Reading, PA) was used to fit plots of

[product] versus time to a single exponential equation: $[\text{product}] = A[1 - \exp(-k_{\text{obs}}t)]$, where A is the amplitude, k_{obs} is the observed first-order rate constant for dTTP or analog incorporation, and t is the reaction time. The k_{obs} values were then plotted against nucleotide concentration to generate k_{pol} , the maximum rate of nucleotide incorporation, and K_d , the dissociation constant for the nucleotide for the enzyme-primer/template substrate complex by fitting to a hyperbolic equation: $k_{\text{obs}} = (k_{\text{pol}} \times [\text{dNTP}])/(K_d + [\text{dNTP}])$, using Kaleidagraph software.

Excision reactions. To incorporate FLT-TP in to the 5'-radiolabeled D22/D45 primer/template substrate, 8.0 μM FLT-TP, 5.0 μM DNA primer/template substrate, 1 μM WT pol γ holoenzyme, and 10 mM MgCl_2 was incubated in pol γ reaction buffer for 3 h at 37°C. For Ed4T-TP incorporation, 30 μM Ed4T-TP, 5.0 μM DNA primer/template substrate, 1.0 μM RT, and 10 mM MgCl_2 was incubated in RT reaction buffer (50 mM Tris, pH 7.8 at 37°C, and 50 mM NaCl) at 37°C for 2 h. The reactions were optimized such that the analog incorporation reaction achieved completion. The remaining experimental parameters were the same for both FLT-MP and Ed4T-MP. The incubations were purified on a 20% denaturing polyacrylamide sequencing gel (8 M urea), and using phosphorimaging, the radiolabeled band, corresponding to the D22 with the analog incorporated at position 23 (D22-FLT-MP or D22-Ed4T-MP) was removed. The DNA was extracted from the gel by gentle mixing at room temperature overnight, in a solution of 0.5 M ammonium acetate, 20 mM magnesium acetate, 1 mM EDTA, and 0.1% SDS. Following ethanol extraction (75% ethanol solution at -80°C for 4 h) and drying, the D22-analog primer was then re-phosphorylated and re-annealed as described previously to generate the DNA primer-analog/template substrate (Ray et al., 2002a). An incubation

of 150 nM exo^+ pol γ holoenzyme and 112 nM DNA primer-analog/template substrate in pol γ reaction buffer was manually mixed with 5 mM MgCl_2 to initiate the excision reaction at 37°C under single-turnover conditions. All concentrations are final, post-mixing. Aliquots of the mixture were removed at various time points and quenched with 0.3 M EDTA (pH 8.0). A 0.4 mm thick 20% denaturing polyacrylamide sequencing gel (8 M urea) was used to separate the products, and phosphorimaging was used to quantitate the loss of substrate. A plot of percent substrate versus time was fit to a single exponential decay equation to generate the rate of excision, k_{exo} . For Ed4T-MP excision, the plot was fit to a Boltzman sigmoidal equation, and the inflection point concentration was used to determine the half-life, which is proportional to k_{exo} under pseudo-first-order kinetics.

Results

Discrimination against FLT-TP and Ed4T-TP by WT pol γ . A critical component of the *in vitro* toxicity profiles for novel NRTIs is the characterization of the extent of incorporation by WT pol γ . Previous work on the interactions of these inhibitors with WT pol γ is limited to an IC_{50} of 2.7 μ M (Cheng et al., 1987) and a K_i of 50 nM (Winska et al., 2010) for FLT-TP, and an IC_{50} value of 100 μ M for Ed4T-TP (100-fold higher than that for d4T-TP (Yang et al., 2007)). Steady-state kinetics only report on the rate-limiting step of catalysis, which for many polymerases, including WT pol γ , is product release, meaning rate constants associated with polymerization cannot be determined from these types of studies. Thus, we used pre-steady-state kinetics to determine the k_{pol} and K_d for FLT-TP and Ed4T-TP incorporation relative to dTTP.

Under single-turnover conditions, WT pol γ holoenzyme and the DNA primer/template substrate were rapidly mixed with $MgCl_2$ and varying concentrations of dTTP, FLT-TP, or Ed4T-TP for varying time points. Triphosphate versions of the drugs were used since the cellular kinases required to phosphorylate the NRTI prodrugs were not present in these *in vitro* studies. Following reaction quenching, the products were separated via gel electrophoresis, and phosphorimaging allowed the quantitation of the single, correct nucleotide incorporation to form the D23 product. The amount of product formed was plotted against the reaction time. This was fit to a single exponential equation to generate the observed rate of nucleotide incorporation, k_{obs} , at each concentration (Fig. 2). These k_{obs} values were then plotted against nucleotide incorporation and fit to a hyperbola to generate k_{pol} and K_d values (Fig. 3).

Unsurprisingly, WT pol γ was able to incorporate dTTP with very high efficiency.

The k_{pol} for FLT-TP incorporation by WT pol γ was ~ 260 -fold slower than for dTTP incorporation (Table 1). However, the affinity for FLT-TP was actually 7.5-fold tighter than that for dTTP, meaning WT pol γ preferred the nucleoside analog based on K_d alone. Because of this, the overall efficiency of FLT-TP incorporation was only 35-fold lower than dTTP incorporation, indicating that FLT-TP may serve as a substrate for WT pol γ *in vivo* to a modest, yet significant extent. This kinetic profile of FLT-TP interaction with WT pol γ is supportive of the evidence of mitochondrial toxicity *in vitro* (de Baar et al., 2007) and *in vivo* (Venhoff et al., 2009).

Interestingly, Ed4T-TP demonstrated a different kinetic mechanism of interaction with WT pol γ than that seen for FLT-TP. The k_{pol} for Ed4T-TP incorporation was 2,100-fold and 7.9-fold slower than dTTP and FLT-TP, respectively (Table 1). Ed4T-TP also showed superiority to FLT-TP in its weak affinity for WT pol γ , with 3-fold and 23-fold increases in K_d versus dTTP and FLT-TP, respectively. Overall, an impressive 6,200-fold and 180-fold drop in incorporation efficiency was seen for Ed4T-TP relative to dTTP and FLT-TP, respectively. This high discrimination against Ed4T-TP indicates that incorporation of this inhibitor in the physiological nucleotide milieu, where individual dNTP concentrations range from low micromolar to sub-millimolar in mammalian (rat) mitochondria (Song et al., 2005; Wheeler and Mathews, 2011), is probably a rare event. This is supported by the findings of low toxicity *in vitro* (Dutschman et al., 2004; Haraguchi et al., 2003; Tanaka et al., 2005).

Discrimination against FLT-TP and Ed4T-TP by RT. The characterization of interaction of these analogs with RT is limited, with previous work including a K_i value of 5 nM for the inhibition of RT by FLT-TP (Cheng et al., 1987), and pre-steady-state

studies showing RT preferred dTTP 1.9-fold over Ed4T-TP, versus a 4.5-fold preference of dTTP over d4T (Yang et al., 2008). We undertook pre-steady-state single-turnover experiments in which RT and the DNA-primer/template substrate were rapidly mixed with MgCl₂ and varying concentrations of dTTP, FLT-TP, or Ed4T-TP (Fig. 4).

A 2.2-fold decrease in k_{pol} and a 2-fold increase in K_d were observed for FLT-TP incorporation by RT relative to dTTP, resulting in a 4.2-fold higher efficiency for dTTP over FLT-TP (Fig. 5, Table 1). Even though there was some preference for the native nucleotide, the similar incorporation efficiency to dTTP indicated that RT would incorporate FLT-TP at significant rates *in vivo*. The k_{pol} for Ed4T-TP incorporation was identical to that of dTTP. Importantly, the binding affinity was tighter as evidenced by the 2-fold decrease in K_d relative to dTTP, indicating that RT incorporated Ed4T-TP 2.0-fold more efficiently than dTTP (Fig. 5, Table 1).

The discrimination by WT pol γ (Table 1) compared favorably to that of RT. RT showed a 8.3-fold loss of discrimination for FLT-TP incorporation relative to WT pol γ , and a striking 12,000-fold decrease in discrimination was seen when comparing Ed4T-TP incorporation by RT to WT pol γ . Thus RT is much more likely to incorporate these inhibitors than WT pol γ . These findings can explain the low toxicity observed thus far for Ed4T-TP, although further clinical testing is still needed.

Excision of FLT-MP and Ed4T-MP by exo^+ pol γ . An important consideration in the *in vitro* toxicity profile of NRTI incorporation by pol γ is the enzyme's inherent proofreading capability. Nucleoside analog incorporation by pol γ can be essentially negated if excision is efficient. Based on nucleoside analog incorporation efficiency, either WT pol γ or RT was used to incorporate a single FLT-TP or a single Ed4T-TP into

the DNA primer/template substrate. The D22-FLT-MP/D45 or D22-Ed4T-MP/D45 primer/template was then used as a substrate in the excision reaction. Under single-turnover conditions, exo^+ pol γ holoenzyme and the DNA primer-analog/template substrate were manually mixed with MgCl_2 , and the reaction was quenched after various time points. After separation of the products using gel electrophoresis and quantitation of the substrate band, the percent of substrate was plotted versus time (Fig. 6) and fit to a single exponential equation to obtain k_{exo} values, and, in the case of Ed4T-MP excision, a sigmoidal equation (Fig. 6B inset).

Both FLT-MP and Ed4T-MP were excised at similar, modest rates, although Ed4T-MP excision is slower based on the sigmoidal fit (Fig. 6). Half-lives for the exo^+ pol γ -D22-analog/D45 complex were 8.8 min and 9.6 min for FLT and Ed4T, respectively. These rates of excision were on average about 34-fold slower than the excision rate of a correctly inserted dT for this primer/template substrate (0.042 s^{-1}) (Feng et al., 2001). However, both analogs were removed more efficiently than ddC and ddA (k_{exo} values of 0.0003 s^{-1} (Hanes and Johnson, 2008) and 0.0005 s^{-1} (Johnson et al., 2001), respectively).

Discrimination against FLT-TP and Ed4T-TP by R964C pol γ . It has been established that d4T-treated patients with the R964C pol γ mutation have higher instances of mitochondrial toxicity (Yamanaka et al., 2007), primarily due to moderate defects in activity and lower nucleoside analog discrimination (Bailey et al., 2009). In order to determine if such alterations in pol γ activity were extended to other dTTP analogs, the single-turnover pre-steady-state experiments with WT pol γ experiments were repeated using the R964C pol γ holoenzyme (Fig. 7). Such studies are important to determine if

patients with the R964C pol γ mutation receiving FLT or Ed4T are at higher risk for mitochondrial toxicity.

The incorporation efficiency of dTTP decreased only slightly (1.4-fold) relative to WT pol γ (Table 1), consistent with the 1.5-fold loss of efficiency measured previously (Bailey et al., 2009). R964C pol γ was able to incorporate FLT-TP with slightly higher efficiency than WT pol γ (1.6-fold higher), and Ed4T-TP was incorporated 2.5-fold more efficiently by R964C pol γ than by WT pol γ (Table 1). When considering the overall discrimination, which takes into account defects in dTTP incorporation, R964C pol γ showed 2.2-fold and 3.4-fold decreases in discrimination against FLT-TP and Ed4T-TP, respectively, relative to WT pol γ (Table 1).

Discussion

The interaction of FLT-TP and Ed4T-TP with WT pol γ and RT were unique, clarifying the reported differences in toxicity. The incorporation efficiency of FLT-TP by WT pol γ was 35-fold slower than dTTP, similar to the more toxic NRTIs on the market, versus the 1,000- to nearly 1 million-fold slower efficiencies for other low toxicity inhibitors (Table 2). This indicates some toxicity stems from FLT-TP incorporation. Further, based on affinity alone, FLT-TP was preferred over dTTP by WT pol γ . Studies examining the potential for toxicity focus on pol γ using the analog as a substrate, but we propose this low K_d indicates the observed mitochondrial toxicity for FLT may also stem from direct inhibition. It is likely to be more complex than simple competition, since it has been shown that FLT-TP is a non-competitive inhibitor of pol γ (Winska et al., 2010). Adding further complexity, it has been proposed that mitochondrial toxicity stems in part from competitive inhibition of host thymidine kinase 2 by FLT (Wang et al., 2011). Thus, it is likely that many factors contribute to FLT toxicity.

Ideally, the discrimination against dNTP analogs by WT pol γ will be high, while the discrimination by RT will be low. This indicates that WT pol γ can readily distinguish among NRTIs and native nucleotides while RT can not. There is only a slight preference for dTTP over FLT-TP by RT, comparing favorably to many FDA-approved NRTIs and inhibitors under development (Table 2). This supports the finding that lower doses of FLT are still effective and less toxic (*vide supra*). WT pol γ very successfully discriminated against Ed4T-TP, showing 6,200- and 180-fold higher discrimination relative to dTTP and FLT-TP incorporation, respectively. This strikingly high selectivity is better than many currently available NRTIs (Table 2). Further, in contrast to the very

high selectivity shown by WT pol γ , RT showed very low discrimination between Ed4T-TP and dTTP. In fact, Ed4T-TP was the preferred substrate. This preference appears to be sequence dependent since a study using a different DNA primer/template substrate found a modest preference for dTTP over Ed4T-TP (Yang et al., 2008).

Importantly, we showed RT was poor at discriminating both Ed4T and d4T from dTTP (discrimination values of 0.51 and 0.56, respectively (Vaccaro et al., 2000), Table 2), and this preference for these two analogs over dTTP is unique among all of the NRTIs assayed to date (Table 2). The didehydro ring found in d4T and Ed4T may help facilitate incorporation by RT and limit the discrimination of these analogs from the native nucleotides. However, while d4T-TP is preferred over dTTP by RT, the corresponding selectivity by WT pol γ is 840-fold lower than for Ed4T-TP (Table 2) (Johnson et al., 2001; Vaccaro et al., 2000). Thus, even though RT prefers both analogs, there is a 13-fold difference in discrimination between RT and WT pol γ for d4T-TP, versus a 12,000-fold difference in discrimination for Ed4T-TP. To our knowledge, Ed4T is the first NRTI to serve both as a preferred substrate for RT and as a nearly negligible substrate for WT pol γ .

Since the only difference between d4T and Ed4T is the presence of the 4'-ethynyl group, this functionality may serve as an enzyme selectivity moiety in that when the ethynyl group is present, discrimination by WT pol γ (but importantly, not RT) improves 840-fold (Table 2). It is likely that a similar trend will be seen with 4'-ethynyl-2-fluoro-2'-deoxyadenosine triphosphate (EFdA-TP), which we found had a 4,300-fold preference for dATP over EFdA (Sohl et al., 2012), and steady-state studies with RT yielded a discrimination of 0.5 (thus EFdA-TP is preferred over dATP) (Michailidis et al., 2009).

NMR spectroscopy studies probing the interaction of RT and EFdA indicated that the 4'-ethynyl group locks the sugar into a conformation favorable for incorporation by RT but not WT pol γ , contributing to the preference of RT for the analog (Kirby et al., 2011). The 4'-ethynyl group may serve as an enzyme selectivity moiety in Ed4T, although structural studies would be required to assess this.

A more subtle characteristic of the poor discrimination shown by RT for FLT-TP and Ed4T-TP concerns the development of resistance. The rate of generation of NRTI resistance mutations in RT following d4T treatment occurs notably more slowly than in other NRTIs (Lin et al., 1994). It has been proposed that this is due, at least in part, to poor discrimination by RT (Ray et al., 2002b; Vaccaro et al., 2000). Thus, our findings of low RT discrimination can offer an explanation for the observed slow RT-resistant mutation rates for FLT and Ed4T (Kim et al., 2001; Nitanda et al., 2005; Yang et al., 2009). We also note that important future work includes testing the incorporation efficiency for FLT-TP and Ed4T-TP by RT containing NRTI-resistant mutation(s) to predict effectiveness in NRTI-experienced patients.

Both FLT-MP and Ed4T-MP were excised somewhat efficiently from the primer/template substrate by exo^+ pol γ (Fig. 6). While a single exponential equation fit the data measured for FLT-MP excision (Fig. 6A) well, a very slight sigmoidal characteristic of Ed4T-MP excision (Fig. 6B) resulted in a minor deviation from a similar fit. This initial slow phase caused a slower rate of excision when using a sigmoidal fit (Fig. 6B inset). It is possible that excision of Ed4T-MP requires a more complicated reaction scheme (i.e., more steps) than FLT-MP excision. This may include conformational change step(s), or changes related to partitioning between the two active

sites. Without structural or spectral evidence to support this, our focus is on the single exponential fit, although experimentally testing alternate reaction schemes are an interest of future study. The rate of dissociation of a DNA template is $\sim 0.02 \text{ s}^{-1}$ (Johnson and Johnson, 2001), so it is likely that DNA dissociation upon dTTP analog incorporation occurs more often than excision.

The moderate excision rates of FLT-MP and Ed4T-MP are within the range of most FDA-approved NRTIs (Johnson et al., 2001) and are more efficient than removal of ddC (0.0003 s^{-1}) (Hanes and Johnson, 2008) and ddA (0.0005 s^{-1}) (Johnson et al., 2001). Our findings of the faster (relative to ddC and ddA) Ed4T excision rate support the work by Hanes and Johnson examining the link between the dissociation constant of the incoming nucleotide analog and the kinetic partitioning of the DNA in the pol γ polymerase and exonuclease active sites (Hanes and Johnson, 2008). Specifically, the low affinity of WT pol γ for Ed4T may facilitate the transfer of the DNA primer/template from the polymerase active site to the exonuclease active site during excision. Affinity constants for ddCTP (Feng et al., 2001) and ddATP (Johnson et al., 2001), which are excised much more slowly by exo^+ pol γ , bind much more tightly than Ed4T. Similarly, the K_d for FLT-TP is an order of magnitude higher than those of ddCTP and ddATP (Johnson et al., 2001), suggesting more favorable excision active site partitioning for FLT removal compared to ddC and ddA to help achieve the faster rate of FLT excision.

As seen with d4T treatment (Yamanaka et al., 2007), we predict patients with the R964C pol γ mutation may show higher instances of mitochondrial toxicity. Like d4T (Bailey et al., 2009), alterations in incorporation kinetics were modest but significant; R964C pol γ incorporated dTTP 1.4-fold less efficiently than WT pol γ , and FLT-TP and

Ed4T-TP were incorporated 1.6-, and 2.5-fold more efficiently, respectively (compared to 2.1-fold more efficiently for d4T-TP (Bailey et al., 2009)) (Table 1). This resulted in an overall 2.2- and 3.4-fold loss of discrimination for dTTP over FLT-TP and Ed4T-TP, respectively (Table 1), similar to the 3.2-fold loss of discrimination for dTTP over d4T-TP determined previously (Bailey et al., 2009). Thus, using these dTTP analogs in patients with the R964C pol γ mutation may lead to higher instances of mitochondrial toxicity due to the similar kinetic profiles seen in d4T (Yamanaka et al., 2007), although it is possible that other toxicity mechanisms may also contribute. This mutation should be taken under consideration when testing FLT and Ed4T in a clinical setting.

In summary, we found that two relatively new RT inhibitors for treatment of HIV infection, FLT-TP and Ed4T-TP, were incorporated by WT pol γ nearly 1 order of magnitude and over 3 orders of magnitude more slowly, respectively, than dTTP. RT, however, readily incorporated both inhibitors, and in fact preferred Ed4T-TP over native nucleotides. Ed4T is the first NRTI shown to be preferred by RT and yet have negligible incorporation by WT pol γ . We propose that the ethynyl group in Ed4T serves as an enzyme selectivity moiety to generate the different discrimination abilities of RT and WT pol γ , an important finding for future NRTI design. These unique kinetic interaction profiles for FLT-TP and Ed4T-TP provide a mechanism to explain the different susceptibilities to toxicity. Such studies are critical in understanding pol γ -mediated mechanisms of toxicity for NRTIs in preclinical and clinical trials.

Acknowledgments

We would like to thank Dr. Ligong Wang for the expression and purification of the WT pol γ accessory subunit.

Authorship Contribution

Participated in research design: Sohl and Anderson.

Conducted experiments: Sohl and Kim.

Contributed new reagents: Kasiviswanathan, Pradere, Schinazi, Copeland, Mitsuya, and Baba.

Performed data analysis: Sohl and Kim.

Wrote or contributed to the writing of the manuscript: Sohl and Anderson.

References

- Apostolova N, Blas-Garcia A and Esplugues JV (2011) Mitochondrial interference by anti-HIV drugs: mechanisms beyond Pol-gamma inhibition. *Trends Pharmacol Sci* **32**(12):715-725.
- Bailey CM, Kasiviswanathan R, Copeland WC and Anderson KS (2009) R964C mutation of DNA polymerase gamma imparts increased stavudine toxicity by decreasing nucleoside analog discrimination and impairing polymerase activity. *Antimicrob Agents Chemother* **53**(6):2610-2612.
- Bienstock RJ and Copeland WC (2004) Molecular insights into NRTI inhibition and mitochondrial toxicity revealed from a structural model of the human mitochondrial DNA polymerase. *Mitochondrion* **4**(2-3):203-213.
- Brinkman K, Smeitink JA, Romijn JA and Reiss P (1999) Mitochondrial toxicity induced by nucleoside-analogue reverse-transcriptase inhibitors is a key factor in the pathogenesis of antiretroviral-therapy-related lipodystrophy. *Lancet* **354**(9184):1112-1115.
- Cheng YC, Dutschman GE, Bastow KF, Sarngadharan MG and Ting RY (1987) Human immunodeficiency virus reverse transcriptase. General properties and its interactions with nucleoside triphosphate analogs. *J Biol Chem* **262**(5):2187-2189.
- de Baar MP, de Rooij ER, Smolders KG, van Schijndel HB, Timmermans EC and Bethell R (2007) Effects of apricitabine and other nucleoside reverse transcriptase inhibitors on replication of mitochondrial DNA in HepG2 cells. *Antiviral Res* **76**(1):68-74.
- De Clercq E (2010) Antiretroviral drugs. *Curr Opin Pharmacol* **10**(5):507-515.

Dutschman GE, Grill SP, Gullen EA, Haraguchi K, Takeda S, Tanaka H, Baba M and Cheng YC (2004) Novel 4'-substituted stavudine analog with improved anti-human immunodeficiency virus activity and decreased cytotoxicity. *Antimicrob Agents Chemother* **48**(5):1640-1646.

Feng JY and Anderson KS (1999) Mechanistic studies comparing the incorporation of (+) and (-) isomers of 3TCTP by HIV-1 reverse transcriptase. *Biochemistry* **38**(1):55-63.

Feng JY, Johnson AA, Johnson KA and Anderson KS (2001) Insights into the molecular mechanism of mitochondrial toxicity by AIDS drugs. *J Biol Chem* **276**(26):23832-23837.

Feng JY, Murakami E, Zorca SM, Johnson AA, Johnson KA, Schinazi RF, Furman PA and Anderson KS (2004) Relationship between antiviral activity and host toxicity: comparison of the incorporation efficiencies of 2',3'-dideoxy-5-fluoro-3'-thiacytidine-triphosphate analogs by human immunodeficiency virus type 1 reverse transcriptase and human mitochondrial DNA polymerase. *Antimicrob Agents Chemother* **48**(4):1300-1306.

Flexner C, van der Horst C, Jacobson MA, Powderly W, Duncanson F, Ganes D, Barditch-Crovo PA, Petty BG, Baron PA, Armstrong D and et al. (1994) Relationship between plasma concentrations of 3'-deoxy-3'-fluorothymidine (alovudine) and antiretroviral activity in two concentration-controlled trials. *J Infect Dis* **170**(6):1394-1403.

Graziewicz MA, Longley MJ, Bienstock RJ, Zeviani M and Copeland WC (2004) Structure-function defects of human mitochondrial DNA polymerase in autosomal

- dominant progressive external ophthalmoplegia. *Nat Struct Mol Biol* **11**(8):770-776.
- Hanes JW and Johnson KA (2008) Exonuclease removal of dideoxycytidine (zalcitabine) by the human mitochondrial DNA polymerase. *Antimicrob Agents Chemother* **52**(1):253-258.
- Haraguchi K, Takeda S, Tanaka H, Nitanda T, Baba M, Dutschman GE and Cheng YC (2003) Synthesis of a highly active new anti-HIV agent 2',3'-didehydro-3'-deoxy-4'-ethynylthymidine. *Bioorg Med Chem Lett* **13**(21):3775-3777.
- Johnson AA and Johnson KA (2001) Exonuclease proofreading by human mitochondrial DNA polymerase. *J Biol Chem* **276**(41):38097-38107.
- Johnson AA, Ray AS, Hanes J, Suo Z, Colacino JM, Anderson KS and Johnson KA (2001) Toxicity of antiviral nucleoside analogs and the human mitochondrial DNA polymerase. *J Biol Chem* **276**(44):40847-40857.
- Johnson AA, Tsai Y, Graves SW and Johnson KA (2000) Human mitochondrial DNA polymerase holoenzyme: reconstitution and characterization. *Biochemistry* **39**(7):1702-1708.
- Kasisviswanathan R, Longley MJ, Young MJ and Copeland WC (2010) Purification and functional characterization of human mitochondrial DNA polymerase gamma harboring disease mutations. *Methods* **51**(4):379-384.
- Kerr SG and Anderson KS (1997) RNA dependent DNA replication fidelity of HIV-1 reverse transcriptase: evidence of discrimination between DNA and RNA substrates. *Biochemistry* **36**(46):14056-14063.

- Kim EY, Vrang L, Oberg B and Merigan TC (2001) Anti-HIV type 1 activity of 3'-fluoro-3'-deoxythymidine for several different multidrug-resistant mutants. *AIDS Res Hum Retroviruses* **17**(5):401-407.
- Kim J, Roberts A, Yuan H, Xiong Y and Anderson KS (2012) Nucleocapsid protein annealing of a primer-template enhances (+)-strand DNA synthesis and fidelity by HIV-1 reverse transcriptase. *J Mol Biol* **415**(5):866-880.
- Kirby KA, Singh K, Michailidis E, Marchand B, Kodama EN, Ashida N, Mitsuya H, Parniak MA and Sarafianos SG (2011) The sugar ring conformation of 4'-ethynyl-2-fluoro-2'-deoxyadenosine and its recognition by the polymerase active site of HIV reverse transcriptase. *Cell Mol Biol (Noisy-le-grand)* **57**(1):40-46.
- Koczor CA and Lewis W (2010) Nucleoside reverse transcriptase inhibitor toxicity and mitochondrial DNA. *Expert Opin Drug Metab Toxicol* **6**(12):1493-1504.
- Kohler JJ and Lewis W (2007) A brief overview of mechanisms of mitochondrial toxicity from NRTIs. *Environ Mol Mutagen* **48**(3-4):166-172.
- Kong XB, Zhu QY, Vidal PM, Watanabe KA, Polsky B, Armstrong D, Ostrander M, Lang SA, Jr., Muchmore E and Chou TC (1992) Comparisons of anti-human immunodeficiency virus activities, cellular transport, and plasma and intracellular pharmacokinetics of 3'-fluoro-3'-deoxythymidine and 3'-azido-3'-deoxythymidine. *Antimicrob Agents Chemother* **36**(4):808-818.
- Lee H, Hanes J and Johnson KA (2003) Toxicity of nucleoside analogues used to treat AIDS and the selectivity of the mitochondrial DNA polymerase. *Biochemistry* **42**(50):14711-14719.

- Lee YS, Kennedy WD and Yin YW (2009) Structural insight into processive human mitochondrial DNA synthesis and disease-related polymerase mutations. *Cell* **139**(2):312-324.
- Lim SE, Ponamarev MV, Longley MJ and Copeland WC (2003) Structural determinants in human DNA polymerase gamma account for mitochondrial toxicity from nucleoside analogs. *J Mol Biol* **329**(1):45-57.
- Lin PF, Samanta H, Rose RE, Patick AK, Trimble J, Bechtold CM, Revie DR, Khan NC, Federici ME, Li H and et al. (1994) Genotypic and phenotypic analysis of human immunodeficiency virus type 1 isolates from patients on prolonged stavudine therapy. *J Infect Dis* **170**(5):1157-1164.
- Longley MJ, Ropp PA, Lim SE and Copeland WC (1998) Characterization of the native and recombinant catalytic subunit of human DNA polymerase gamma: identification of residues critical for exonuclease activity and dideoxynucleotide sensitivity. *Biochemistry* **37**(29):10529-10539.
- Michailidis E, Marchand B, Kodama EN, Singh K, Matsuoka M, Kirby KA, Ryan EM, Sawani AM, Nagy E, Ashida N, Mitsuya H, Parniak MA and Sarafianos SG (2009) Mechanism of inhibition of HIV-1 reverse transcriptase by 4'-ethynyl-2'-fluoro-2'-deoxyadenosine triphosphate, a translocation-defective reverse transcriptase inhibitor. *J Biol Chem* **284**(51):35681-35691.
- Mitsuya H, Weinhold KJ, Furman PA, St Clair MH, Lehrman SN, Gallo RC, Bolognesi D, Barry DW and Broder S (1985) 3'-Azido-3'-deoxythymidine (BW A509U): an antiviral agent that inhibits the infectivity and cytopathic effect of human T-

lymphotropic virus type III/lymphadenopathy-associated virus *in vitro*. *Proc Natl Acad Sci USA* **82**(20):7096-7100.

Murakami E, Basavapathruni A, Bradley WD and Anderson KS (2005) Mechanism of action of a novel viral mutagenic covert nucleotide: molecular interactions with HIV-1 reverse transcriptase and host cell DNA polymerases. *Antiviral Res* **67**(1):10-17.

Murakami E, Feng JY, Lee H, Hanes J, Johnson KA and Anderson KS (2003) Characterization of novel reverse transcriptase and other RNA-associated catalytic activities by human DNA polymerase gamma: importance in mitochondrial DNA replication. *J Biol Chem* **278**(38):36403-36409.

Nitanda T, Wang X, Kumamoto H, Haraguchi K, Tanaka H, Cheng YC and Baba M (2005) Anti-human immunodeficiency virus type 1 activity and resistance profile of 2',3'-didehydro-3'-deoxy-4'-ethynylthymidine *in vitro*. *Antimicrob Agents Chemother* **49**(8):3355-3360.

Paintsil E, Dutschman GE, Hu R, Grill SP, Lam W, Baba M, Tanaka H and Cheng YC (2007) Intracellular metabolism and persistence of the anti-human immunodeficiency virus activity of 2',3'-didehydro-3'-deoxy-4'-ethynylthymidine, a novel thymidine analog. *Antimicrob Agents Chemother* **51**(11):3870-3879.

Ray AS, Basavapathruni A and Anderson KS (2002a) Mechanistic studies to understand the progressive development of resistance in human immunodeficiency virus type 1 reverse transcriptase to abacavir. *J Biol Chem* **277**(43):40479-40490.

Ray AS, Murakami E, Peterson CN, Shi J, Schinazi RF and Anderson KS (2002b) Interactions of enantiomers of 2',3'-didehydro-2',3'-dideoxy-fluorocytidine with

- wild type and M184V mutant HIV-1 reverse transcriptase. *Antiviral Res* **56**(3):189-205.
- Ray AS, Schinazi RF, Murakami E, Basavapathruni A, Shi J, Zorca SM, Chu CK and Anderson KS (2003) Probing the mechanistic consequences of 5-fluorine substitution on cytidine nucleotide analogue incorporation by HIV-1 reverse transcriptase. *Antivir Chem Chemother* **14**(3):115-125.
- Ray AS, Yang Z, Shi J, Hobbs A, Schinazi RF, Chu CK and Anderson KS (2002c) Insights into the molecular mechanism of inhibition and drug resistance for HIV-1 RT with carbovir triphosphate. *Biochemistry* **41**(16):5150-5162.
- Sohl CD, Singh K, Kasiviswanathan R, Copeland WC, Mitsuya H, Sarafianos SG and Anderson KS (2012) Mechanism of interaction of human mitochondrial DNA polymerase gamma with the novel nucleoside reverse transcriptase inhibitor 4'-ethynyl-2-fluoro-2'-deoxyadenosine indicates a low potential for host toxicity. *Antimicrob Agents Chemother* **56**(3):1630-1634.
- Song S, Pursell ZF, Copeland WC, Longley MJ, Kunkel TA and Mathews CK (2005) DNA precursor asymmetries in mammalian tissue mitochondria and possible contribution to mutagenesis through reduced replication fidelity. *Proc Natl Acad Sci USA* **102**(14):4990-4995.
- Tanaka H, Haraguchi K, Kumamoto H, Baba M and Cheng YC (2005) 4'-Ethynylstavudine (4'-Ed4T) has potent anti-HIV-1 activity with reduced toxicity and shows a unique activity profile against drug-resistant mutants. *Antivir Chem Chemother* **16**(4):217-221.

- Vaccaro JA and Anderson KS (1998) Implication of the tRNA initiation step for human immunodeficiency virus type 1 reverse transcriptase in the mechanism of 3'-azido-3'-deoxythymidine (AZT) resistance. *Biochemistry* **37**(40):14189-14194.
- Vaccaro JA, Parnell KM, Terezakis SA and Anderson KS (2000) Mechanism of inhibition of the human immunodeficiency virus type 1 reverse transcriptase by d4TTP: an equivalent incorporation efficiency relative to the natural substrate dTTP. *Antimicrob Agents Chemother* **44**(1):217-221.
- Venhoff AC, Lebrecht D, Reuss FU, Heckl-Ostreicher B, Wehr R, Walker UA and Venhoff N (2009) Mitochondrial DNA depletion in rat liver induced by foslovudine tidoxil, a novel nucleoside reverse transcriptase inhibitor prodrug. *Antimicrob Agents Chemother* **53**(7):2748-2751.
- Wang L, Sun R and Eriksson S (2011) The kinetic effects on thymidine kinase 2 by enzyme-bound dTTP may explain the mitochondrial side effects of antiviral thymidine analogs. *Antimicrob Agents Chemother* **55**(6):2552-2558.
- Wheeler LJ and Mathews CK (2011) Nucleoside triphosphate pool asymmetry in mammalian mitochondria. *J Biol Chem* **286**(19):16992-16996.
- Winska P, Miazga A, Poznanski J and Kulikowski T (2010) Partial selective inhibition of HIV-1 reverse transcriptase and human DNA polymerases gamma and beta by thiated 3'-fluorothymidine analogue 5'-triphosphates. *Antiviral Res* **88**(2):176-181.
- Yamanaka H, Gatanaga H, Kosalaraksa P, Matsuoka-Aizawa S, Takahashi T, Kimura S and Oka S (2007) Novel mutation of human DNA polymerase gamma associated with mitochondrial toxicity induced by anti-HIV treatment. *J Infect Dis* **195**(10):1419-1425.

- Yang G, Dutschman GE, Wang CJ, Tanaka H, Baba M, Anderson KS and Cheng YC (2007) Highly selective action of triphosphate metabolite of 4'-ethynyl D4T: a novel anti-HIV compound against HIV-1 RT. *Antiviral Res* **73**(3):185-191.
- Yang G, Paintsil E, Dutschman GE, Grill SP, Wang CJ, Wang J, Tanaka H, Hamasaki T, Baba M and Cheng YC (2009) Impact of novel human immunodeficiency virus type 1 reverse transcriptase mutations P119S and T165A on 4'-ethynylthymidine analog resistance profile. *Antimicrob Agents Chemother* **53**(11):4640-4646.
- Yang G, Wang J, Cheng Y, Dutschman GE, Tanaka H, Baba M and Cheng YC (2008) Mechanism of inhibition of human immunodeficiency virus type 1 reverse transcriptase by a stavudine analogue, 4'-ethynyl stavudine triphosphate. *Antimicrob Agents Chemother* **52**(6):2035-2042.

Footnotes

This work was supported by the National Institutes of Health [GM049551, GM099289, and CFAR 2P30-AI-050409], by the Intramural Research Program of the National Institutes of Health, NIEHS [ES065080], and by the Atlanta Department of Veteran Affairs.

Figure Legends

Figure 1. Structures of dT analogs.

Figure 2. Observed rates of incorporation of dTTP or dTTP analogs opposite dA by WT pol γ . Each point in the plot represents a single observation, and single exponential equations were used to fit the kinetic traces at varying concentrations of dTTP or dTTP analog. These 6-8 experiments all contribute to the k_{pol} and K_d rate constants. (A)

Incorporation of dTTP. Concentrations of dTTP are denoted as follows: $\text{---}\bullet\text{---}$ = 0.20 μM , $\text{---}\triangle\text{---}$ = 0.40 μM , $\text{---}\blacksquare\text{---}$ = 0.80 μM , $\text{---}\times\text{---}$ = 1.5 μM , $\text{---}\square\text{---}$ = 3.0 μM , $\text{---}\blacktriangledown\text{---}$ = 6.0 μM , $\text{---}\blacklozenge\text{---}$ = 8 μM , $\text{---}+\text{---}$ = 13 μM , $\text{---}\boxminus\text{---}$ = 20 μM . (B) Incorporation of FLT-TP.

Concentrations of FLT-TP are denoted as follows: $\text{---}\bullet\text{---}$ = 0.10 μM , $\text{---}\triangle\text{---}$ = 0.25 μM , $\text{---}\blacksquare\text{---}$ = 0.50 μM , $\text{---}\times\text{---}$ = 1.0 μM , $\text{---}\square\text{---}$ = 2.0 μM , $\text{---}\blacktriangledown\text{---}$ = 5.0 μM , $\text{---}\blacklozenge\text{---}$ = 8.0 μM . (C) Incorporation of Ed4T-TP. Concentrations of Ed4T-TP are denoted as follows:

$\text{---}\bullet\text{---}$ = 1.5 μM , $\text{---}\triangle\text{---}$ = 2.5 μM , $\text{---}\blacksquare\text{---}$ = 5.0 μM , $\text{---}\times\text{---}$ = 8.0 μM , $\text{---}\square\text{---}$ = 10 μM , $\text{---}\blacktriangledown\text{---}$ = 20 μM , $\text{---}\blacklozenge\text{---}$ = 30 μM , $\text{---}+\text{---}$ = 40 μM , $\text{---}\boxminus\text{---}$ = 50 μM , $\text{---}\blacktriangle\text{---}$ = 75 μM .

Figure 3. The observed rate of incorporation of dTTP analogs opposite dA by WT pol γ is dependent on nucleotide concentration. Hyperbolic equations were used to fit plots of the observed rate constants generated from Fig. 2 plotted against dTTP analog concentration to obtain k_{pol} and K_d values. Each point in the graphs represents the

observed rate generated from Fig. 2, and the standard error is from deviance from the hyperbolic fits. See Table 1 for k_{pol} , K_d , and efficiency values. (A) Incorporation of dTTP. (B) Incorporation of FLT-TP. (C) Incorporation of Ed4T.

Figure 4. Observed rates of incorporation of dTTP or dTTP analogs opposite dA by RT. Each point in the plot represents a single observation, and single exponential equations were used to fit the kinetic traces at varying concentrations of dTTP or dTTP analog. These 6-8 experiments all contribute to the k_{pol} and K_d rate constants. (A) Incorporation of dTTP. Concentrations of dTTP are denoted as follows: —●— = 0.50 μ M, ---△--- = 1.0 μ M, —■— = 2.0 μ M, ---×--- = 4.0 μ M, —□— = 10 μ M, ---▼--- = 20 μ M. (B) Incorporation of FLT-TP. Concentrations of FLT-TP are denoted as follows: —●— = 0.50 μ M, ---△--- = 2.0 μ M, —■— = 5.0 μ M, ---×--- = 8.0 μ M, —□— = 10 μ M, ---▼--- = 12 μ M, —◆— = 16 μ M, ---+--- = 20 μ M. (C) Incorporation of Ed4T-TP. Concentrations of Ed4T-TP are denoted as follows: —●— = 0.20 μ M, ---△--- = 0.60 μ M, —■— = 1.0 μ M, ---×--- = 1.4 μ M, —□— = 1.8 μ M, ---▼--- = 2.0 μ M, —◆— = 8.0 μ M, ---+--- = 20 μ M.

Figure 5. The observed rate of incorporation of dTTP analogs opposite dA by RT is dependent on nucleotide concentration. Hyperbolic equations were used to fit plots of the observed rate constants (generated from Fig. 4) versus dTTP analog concentration to

obtain k_{pol} and K_{d} values. Each point in the graphs represents the observed rate generated from Fig. 4, and the standard error is from deviance from the hyperbolic fits. See Table 1 for k_{pol} , K_{d} , and efficiency values. **(A)** Incorporation of dTTP. **(B)** Incorporation of FLT-TP. **(C)** Incorporation of Ed4T.

Figure 6. Rates of dTTP analog excision by exo^+ pol γ . Single exponential decay equations were used to determine k_{exo} values. **(A)** Excision of FLT-MP. $k_{\text{exo}} = 0.00130 \pm 0.00005 \text{ s}^{-1}$. **(B)** Excision of Ed4T-MP. $k_{\text{exo}} = 0.0012 \pm 0.0002 \text{ s}^{-1}$. The inset shows a sigmoidal fit of the data. Here, $k_{\text{exo}} = 0.00018 \text{ s}^{-1}$.

Figure 7. The observed rate of incorporation of dTTP analogs opposite dA by R964C pol γ is dependent on nucleotide concentration. Hyperbolic equations were used to fit plots of the observed rate constants versus dTTP analog concentration to obtain k_{pol} and K_{d} values. Each point in the graphs represents the observed rate generated from fitting a time course with 10 different points using a single exponential expression, and the standard error is from deviance from the hyperbolic fits. See Table 1 for k_{pol} , K_{d} , and efficiency values. **(A)** Incorporation of dTTP. **(B)** Incorporation of FLT-TP. **(C)** Incorporation of Ed4T.

Tables

Table 1. Kinetic parameters for WT pol γ , RT, and R964C pol γ

Enzyme	dTTP analog	$k_{\text{pol}}, \text{s}^{-1}$	$K_{\text{d}}, \mu\text{M}$	Efficiency ^a , $\mu\text{M}^{-1} \text{s}^{-1}$	Discrimination, $\text{efficiency}_{\text{dTTP}}/$ $\text{efficiency}_{\text{analog}}$
WT pol γ	dTTP	147 ± 12	3.0 ± 0.8	49	NA ^b
WT pol γ	FLT-TP	0.56 ± 0.03	0.40 ± 0.08	1.4	35
WT pol γ	Ed4T-TP	0.071 ± 0.003	9 ± 1	0.0079	6,200
RT	dTTP	1.25 ± 0.06	3.0 ± 0.4	0.42	NA
RT	FLT-TP	0.58 ± 0.05	6 ± 1	0.1	4.2
RT	Ed4T-TP	1.25 ± 0.05	1.5 ± 0.2	0.83	0.51
R964C pol γ	dTTP	129 ± 8	3.7 ± 0.7	35	NA
R964C pol γ	FLT-TP	0.51 ± 0.03	0.23 ± 0.06	2.2	16
R964C pol γ	Ed4T-TP	0.11 ± 0.01	7 ± 2	0.02	1,800

^a Efficiency = $k_{\text{pol}}/K_{\text{d}}$

^b Not applicable

Table 2. Comparison of incorporation efficiency of nucleoside analogs by WT pol γ and RT with FDA-approved NRTIs and NRTIs under development^a

dNTP analog	WT pol γ discrimination ^b	RT discrimination	Reference
ddCTP	2.9	10	(Feng and Anderson, 1999; Feng et al., 2001; Ray et al., 2003)
ddATP	4.0	5	(Johnson et al., 2001)
d4T-TP	7.4	0.56	(Johnson et al., 2001; Vaccaro et al., 2000)
KP1212-TP	26	14	(Murakami et al., 2005)
FLT-TP	35	4.2	This work
(-) 3TC-TP	2,900	40	(Feng and Anderson, 1999; Feng et al., 2001; Ray et al., 2003)
EFdA-TP	4,300	ND ^{c, d}	(Sohl et al., 2012)
Ed4T-TP	6,200	0.51	This work
PMPApp	11,400	6.1	(Johnson et al., 2001)

AZT-TP	37,000	2.7	(Johnson et al., 2001; Vaccaro and Anderson, 1998)
(-) FTC-TP	290,000	16	(Feng et al., 2004)
CBV-TP	900,000	34	(Johnson et al., 2001)

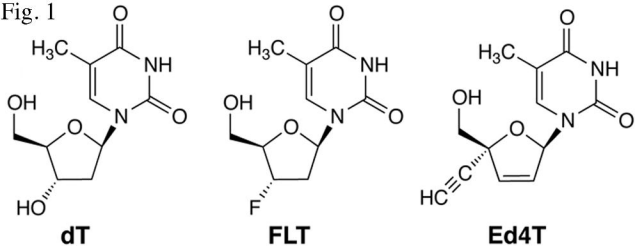
^a Discrimination, rather than incorporation efficiency, is shown to minimize the rate constant variations associated with different primer/template substrates.

^b $\text{Efficiency}_{\text{dNTP}}/\text{efficiency}_{\text{analog}}$

^c ND, No data

^d Steady-state studies indicate an efficiency of 0.5 (Michailidis et al., 2009).

Fig. 1



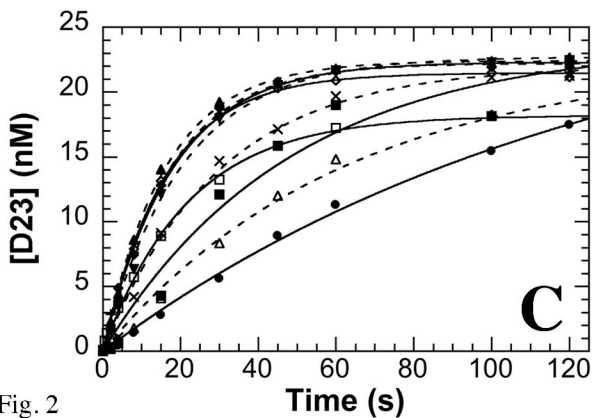
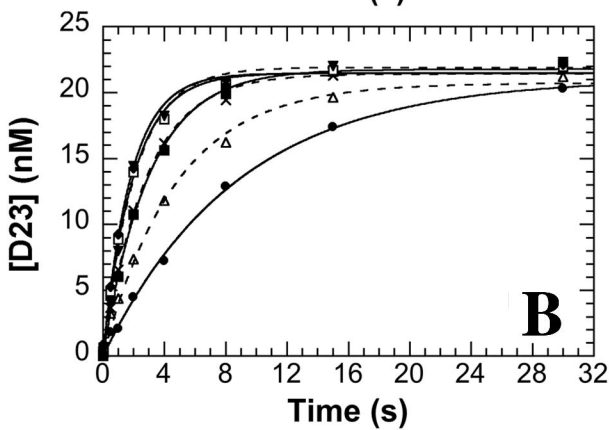
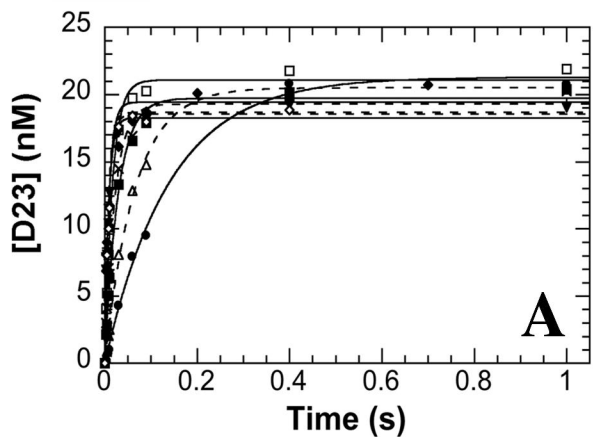


Fig. 2

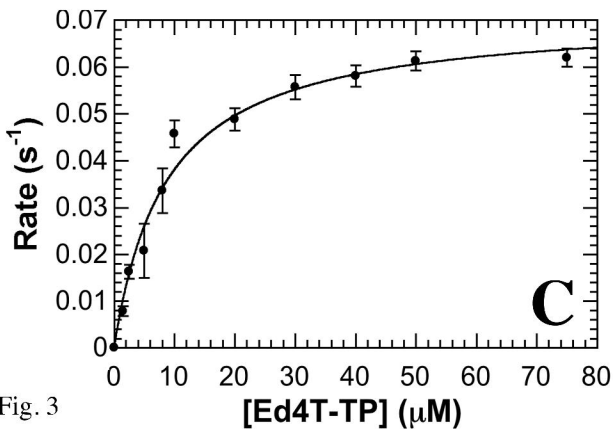
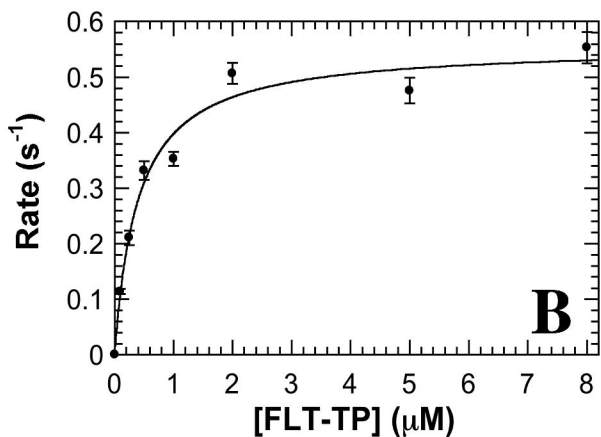
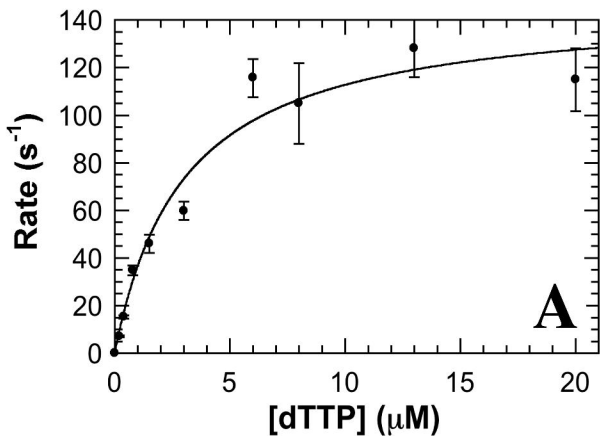


Fig. 3

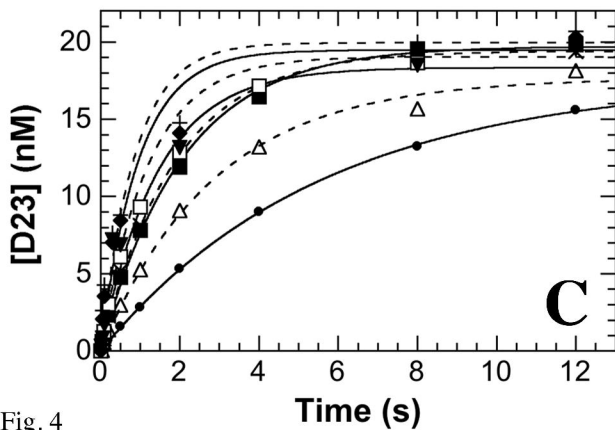
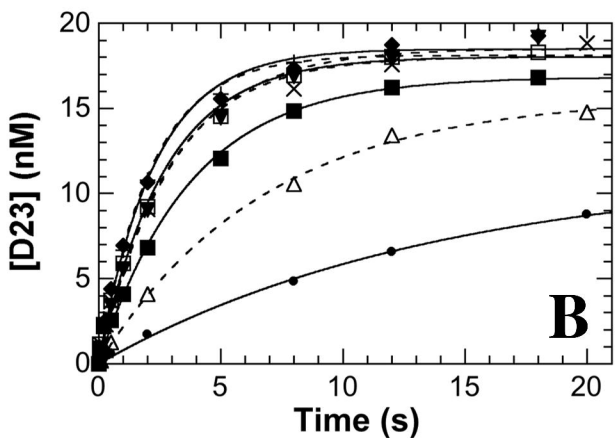
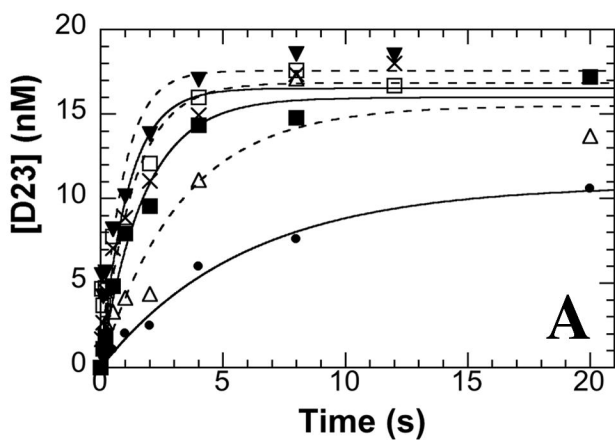


Fig. 4

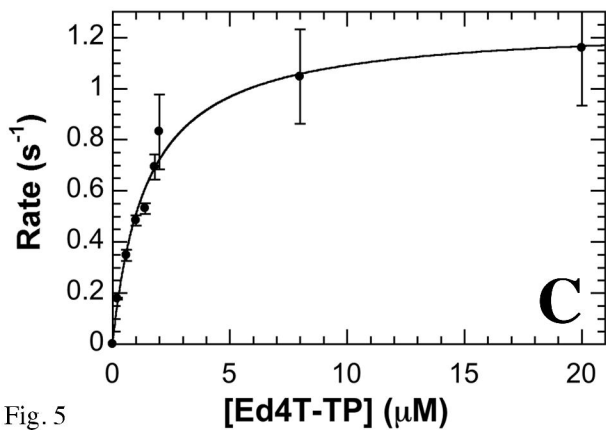
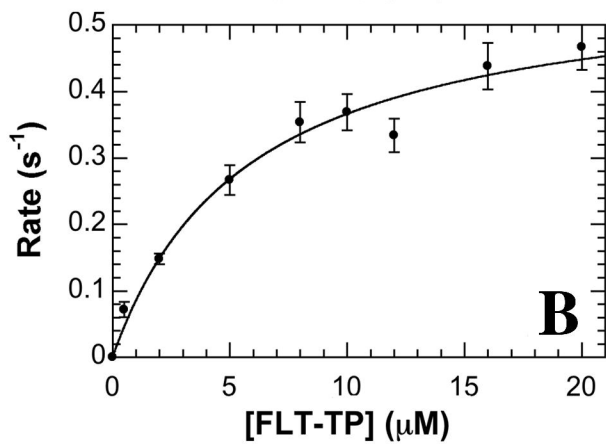
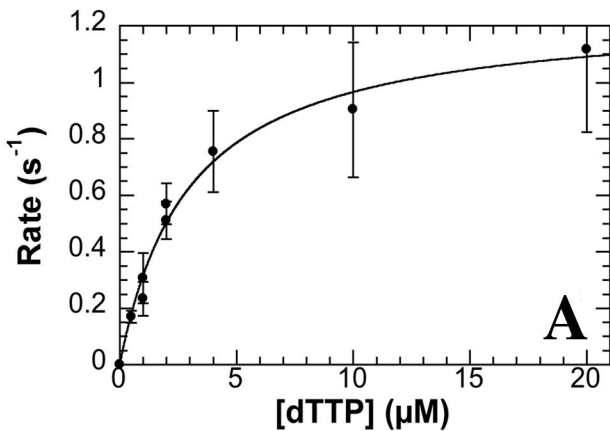


Fig. 5

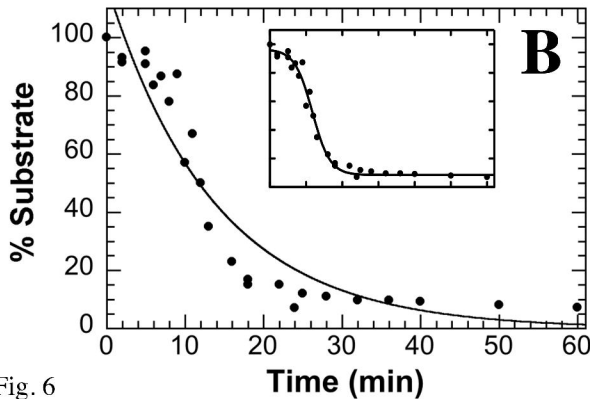
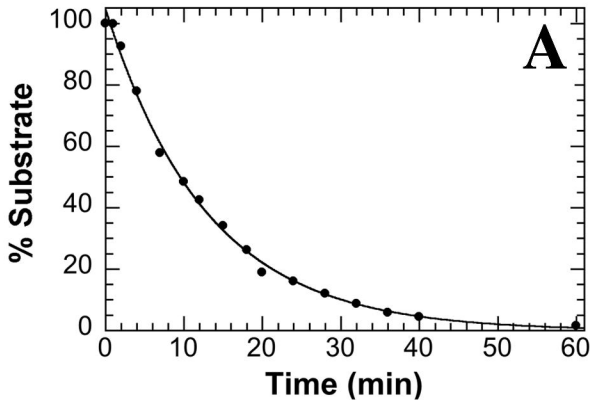


Fig. 6

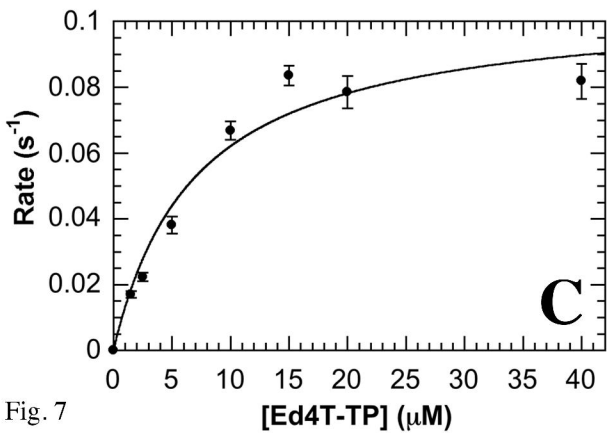
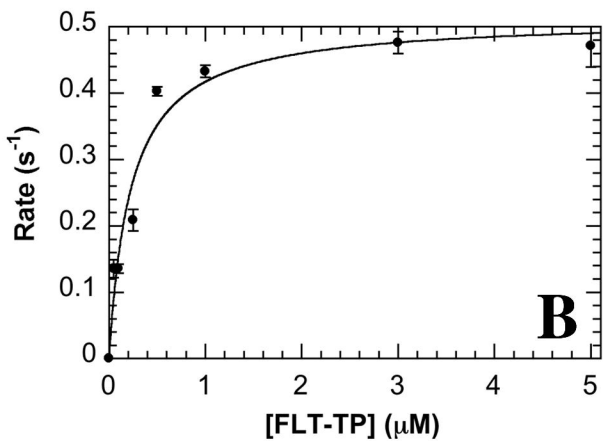
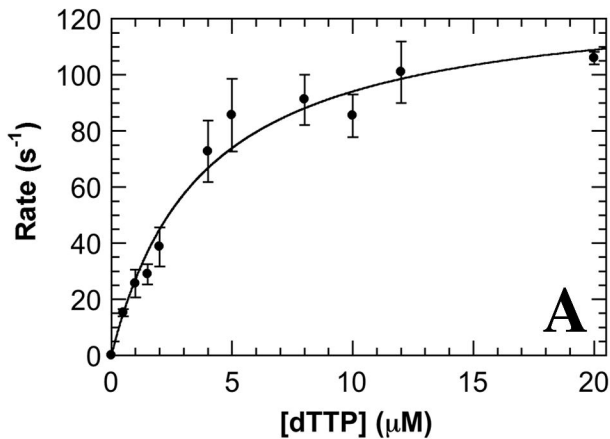


Fig. 7